

Article

# Pulmonary Lymphangitis Poses a Major Challenge for Radiologists in an Oncological Setting during the COVID-19 Pandemic

Roberta Fusco<sup>1</sup>, Igino Simonetti<sup>2</sup>, Stefania Ianniello<sup>3</sup>, Alberta Villanacci<sup>3</sup>, Francesca Grassi<sup>4</sup>, Federica Dell'Aversana<sup>4</sup>, Roberta Grassi<sup>4,5</sup>, Diletta Cozzi<sup>5,6</sup>, Eleonora Bicci<sup>5,6</sup>, Pierpaolo Palumbo<sup>7</sup> , Alessandra Borgheresi<sup>5,8</sup> , Andrea Giovagnoni<sup>5,8</sup>, Vittorio Miele<sup>5,6</sup> , Antonio Barile<sup>9</sup>  and Vincenza Granata<sup>2,\*</sup> 

- <sup>1</sup> Medical Oncology Division, Igea SpA, 80013 Napoli, Italy; r.fusco@igeamedical.com
- <sup>2</sup> Division of Radiology, Istituto Nazionale Tumori IRCCS Fondazione Pascale—IRCCS di Napoli, 80131 Naples, Italy; igino.simonetti@istitutotumori.na.it
- <sup>3</sup> Diagnostica per Immagini nelle Malattie Infettive INMI Spallanzani IRCCS, 00161 Rome, Italy; stefania.ianniello@inmi.it (S.I.); alberta.villanacci@inmi.it (A.V.)
- <sup>4</sup> Division of Radiology, Università degli Studi della Campania Luigi Vanvitelli, 80127 Naples, Italy; francescagrassi1996@gmail.com (F.G.); federica.dellaversana@studenti.unicampania.it (F.D.); grassi.roberta89@gmail.com (R.G.)
- <sup>5</sup> Italian Society of Medical and Interventional Radiology (SIRM), SIRM Foundation, Via della Signora 2, 20122 Milan, Italy; cozzid@aou-careggi.toscana.it (D.C.); eleonora.bicci92@gmail.com (E.B.); alessandra.borgheresi@gmail.com (A.B.); a.giovagnoni@univpm.it (A.G.); vmiele@sirm.org (V.M.)
- <sup>6</sup> Department of Radiology, Azienda Ospedaliero-Universitaria Careggi, 50134 Florence, Italy
- <sup>7</sup> Abruzzo Health Unit 1, Department of Diagnostic Imaging, Area of Cardiovascular and Interventional Imaging, 67100 L'Aquila, Italy; palumbopierpaolo89@gmail.com
- <sup>8</sup> Department of Clinical, Special and Dental Sciences, Marche Polytechnic University, 60126 Ancona, Italy
- <sup>9</sup> Department of Applied Clinical Science and Biotechnology, University of L'Aquila, Via Vetoio 1, 67100 L'Aquila, Italy; antonio.barile@univaq.it
- \* Correspondence: v.granata@istitutotumori.na.it



**Citation:** Fusco, R.; Simonetti, I.; Ianniello, S.; Villanacci, A.; Grassi, F.; Dell'Aversana, F.; Grassi, R.; Cozzi, D.; Bicci, E.; Palumbo, P.; et al. Pulmonary Lymphangitis Poses a Major Challenge for Radiologists in an Oncological Setting during the COVID-19 Pandemic. *J. Pers. Med.* **2022**, *12*, 624. <https://doi.org/10.3390/jpm12040624>

Academic Editors: Attilio A. M. Bianchi and Franco M. Buonaguro

Received: 13 March 2022

Accepted: 31 March 2022

Published: 12 April 2022

**Publisher's Note:** MDPI stays neutral with regard to jurisdictional claims in published maps and institutional affiliations.



**Copyright:** © 2022 by the authors. Licensee MDPI, Basel, Switzerland. This article is an open access article distributed under the terms and conditions of the Creative Commons Attribution (CC BY) license (<https://creativecommons.org/licenses/by/4.0/>).

**Abstract:** Due to the increasing number of COVID-19-infected and vaccinated individuals, radiologists continue to see patients with COVID-19 pneumonitis and recall pneumonitis, which could result in additional workups and false-positive results. Moreover, cancer patients undergoing immunotherapy may show therapy-related pneumonitis during imaging management. This is otherwise known as immune checkpoint inhibitor-related pneumonitis. Following on from this background, radiologists should seek to know their patients' COVID-19 infection and vaccination history. Knowing the imaging features related to COVID-19 infection and vaccination is critical to avoiding misleading results and alarmism in patients and clinicians.

**Keywords:** pulmonary lymphangitis; COVID 19; vaccination; computed tomography

## 1. Background

The current coronavirus disease 2019 (COVID-19) pandemic caused by severe acute respiratory syndrome coronavirus 2 (SARS-CoV-2) has produced a worldwide public health threat with millions of people at risk [1–10]. Globally, as of 5:18 PM CET on 4 March 2022, there were 440,807,756 confirmed cases of COVID-19, including 5,978,096 deaths, reported to the World Health Organization (WHO). In Italy, from 3 January 2020 at 5:18 p.m. CET to 4 March 2022, 12,910,506 confirmed cases of COVID-19 with 155,399 deaths have been registered, reported to the WHO [11].

The symptoms of COVID-19 infection are different from patient to patient, with the most common including fever, fatigue, cough, anorexia, and shortness of breath during different phases of this disease [12–14]. Additionally, less common symptoms such as a

sore throat, headache, confusion, and chest tightness have been also observed [15,16], as well as minor gastrointestinal complications such as nausea, vomiting, and diarrhoea [17]. However, there have been patients not yet symptomatic (pre-symptomatic) and there have been patients without symptoms typical of the COVID-19 disease (asymptomatic), as revealed in several reports [18–20]. Several patients with COVID-19 infection were asymptomatic throughout the infection period [21,22]. In these asymptomatic patients the diagnosis was often accidental, as they performed radiological examinations for another cause or during the follow-up periods when dealing with cancer patients [23–32].

In addition, it has been critical to develop a vaccine as soon as possible to prevent SARS-CoV-2 infection in order to safeguard persons who are at a high risk of complications. Globally, on 27 February 2022, a total of 10,585,766,316 vaccine doses had been administered [11]. The Italian government employed the subsequent vaccination policy: two vaccine doses, with a booster dose 5–6 months after the end of the vaccination cycle, in patients who have not been infected. A policy for assessing vaccine adverse events is founded on the collaboration of local and national health structures, assisted by the Italian Medicines Agency (AIFA) [33]. Since the inception of vaccine inoculation, several adverse events have been reported and shared world-wide, with different findings reported by imaging studies [34–44]. While COVID-19-vaccine-related lymphadenopathy (LAP) has been gradually reported [34], few studies have reported lymphangitis after vaccination from COVID-19, and in several patients, radiation recall pneumonitis has been reported [45–55].

Since during the imaging management of oncological patients, the lung remains as the site of metastases, with different findings, including lymphangitis pattern [56–61], as well as the site of adverse events such as pneumonitis related to such therapies as Immune Checkpoint Inhibitor-Related Pneumonitis [62–70], it is clear that radiologists should know of previous COVID-19 infection or vaccination. The knowledge of these features related to COVID-19 infection or vaccination is critical in order to not presenting misleading results in patients and clinicians by determining disease progression or an adverse treatment effect.

This narrative review aims to evaluate the different patterns of pulmonary lymphangitis to improve the knowledge.

#### *Pulmonary Lymphangitis Carcinomatosa*

Pulmonary lymphangitis carcinomatosa (PLC) is an unusual appearance of metastatic lung disease in which advanced cancers spread through pulmonary lymphatic vessels (Figure 1).

The difficult outflow of lymph from the lungs causes accumulation of interstitial fluid and disturbances in the diffusion of oxygen, which can cause respiratory dysfunction.

Imaging findings appear later than symptoms, and dyspnoea, representing the most frequent symptom, is habitually more severe than radiological findings [56–58]. The most common primary cancers that coexist with PLC are breast (17.3%), lung (10.8%) and stomach (10.8%) cancers [56]. According to Bruce et al. [70], the prevalence of PLC ranges from 6% to 8% in patients with malignant disease. Kazawa et al. [71] showed that the prevalence of PLC-related small-cell lung cancer was recognized in 8.8%. In patients with cancer and pulmonary embolism, the prevalence of PLC was 4.5% [72–77].

There are several hypotheses regarding the metastatic tumour spread, mainly limited to the lymphatics, although the precise process is still uncertain. The tumour could spread through the haematogenous route, causing obliterated endarteritis and then penetrating the vascular endothelium to reach the perivascular lymphatics, to remain stationed there. Direct entry into lymphatic circulation is possible when nearby lymph vessels are involved. Trans-diaphragmatic diffusion has also been suggested to clarify PLC due to abdominal cancers. Local obstruction and fluid accumulation follow soon after the malignant cells are trapped in the lymphatic vessels. This is followed by thickening of the bronchovascular bundles and alveolar septa due to tissue oedema and nodular thickening, suggesting local tumour cell growth.

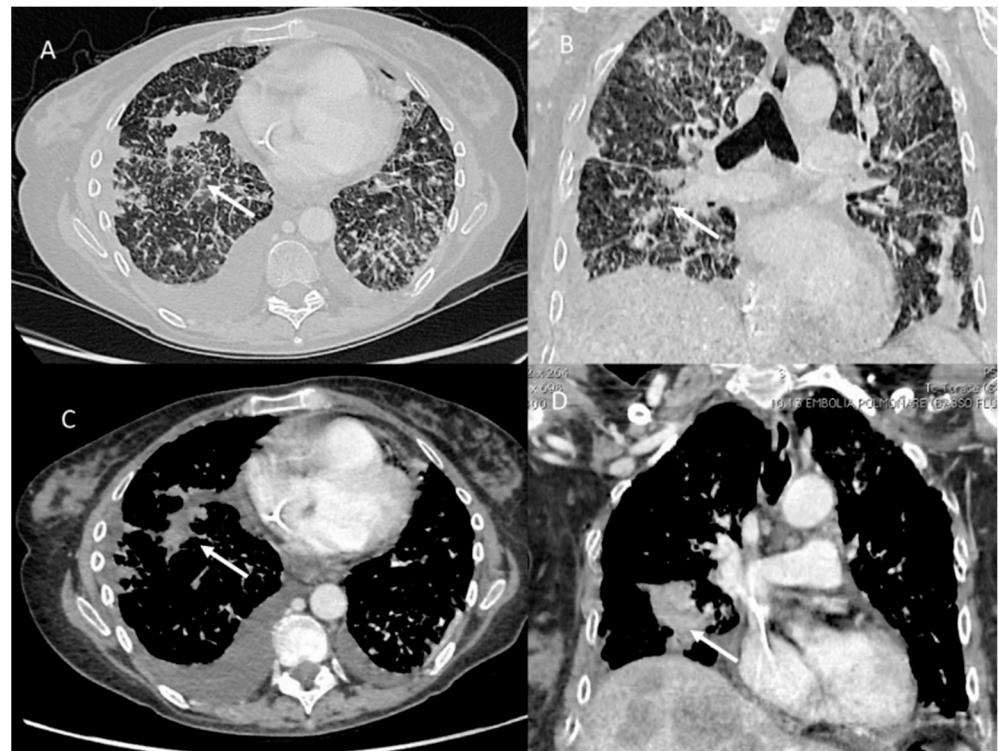


**Figure 1.** PLC in pancreatic cancer patient. CT (axial (A,C) and coronal (B,D)) shows comprise diffuse intrapulmonary infiltrates (arrows) with irregularly interlobular septal thickening, nodular thickening and pleural effusions.

Imaging has low specificity for PLC detection because images are often normal in initial phases. However, imaging is often performed to rule out other causes [57,78–85]. A chest radiograph (chest X-ray) may be the first approach and an association of several radiological findings could favour the diagnosis in about half the cases. However, in 30 to 50% of patients, especially in the initial phases, the X-ray may be normal [56,57]. Therefore, computed tomography (CT) and especially high-resolution CT (HRCT) are recommended techniques for studying patients with suspected PLC [55–57,86–93]. The CT results are similar to other interstitial lung diseases, so they have low diagnostic accuracy in differentiating and detecting PLC [56,57]. The usual CT findings comprise nodular or diffuse intrapulmonary infiltrates, irregularly interlobular septal thickening, smooth (early stage) or nodular thickening (late development), hilar and mediastinal lymphadenopathy, ground-glass opacity due to interstitial oedema or parenchymal extension of tumours, and pleural effusions. These features could be on one or both sides, focal or diffuse, or symmetrical or asymmetrical. Smooth or irregularly thickened interlobular septae are more conducive to PLC than to tumour embolism. Although nodular thickening of the septae is thought to differentiate PLC from other interstitial lung patterns, some conditions such as sarcoidosis or asbestosis may mimic it [57]. Another distinguishing feature of PLC is the preservation of the general and lobular architecture of the lung. [56,57].

## 2. Immune Checkpoint Inhibitor-Related Pneumonitis

Anti-programmed death-1 (anti-PD-1) and programmed anti-death ligand 1 (anti-PD-L1) monoclonal antibodies (mAb) for patients with multiple cancers are licensed treatments, including nivolumab and pem-brolizumab for melanoma and non-small-cell lung cancer (NSCLC), nivolumab for renal cell carcinoma and Hodgkin’s lymphoma, atezolizumab for bladder cancer, and nivolumab plus ipilimumab for melanoma [94–103]. A major feature of anti-PD-1/PD-L1 mAbs is their mild toxicity, but serious immune-related adverse events can occur. Pneumonia is an immune-related adverse event defined as focal or diffuse inflammation of the lung parenchyma, and its incidence in studies with anti-PD-1/PD-L1 mAbs

ranges from 0% to 10% [104]. Drug-related pneumonia can also occur with chemotherapy (docetaxel [105], gemcitabine [106], bleomycin [107]), targeted therapy (epidermal growth factor receptor inhibitors [108,109], mammalian target of rapamycin inhibitors [110]), and radiotherapy [111,112].

Compared to conventional chemotherapy for pneumonia, these patients showed a greater susceptibility to the development of treatment-related pneumonia, with an increased risk of high-grade pneumonia. Previous studies on this pneumonia have shown that clinical, radiological and pathological characterization can facilitate early diagnosis to improve patient outcomes [113–117]. The aetiology and underlying mechanisms of anti-PD-1/PD-L1 mAb-associated pneumonia are unknown [63,118–121].

Immune checkpoint inhibitor (ICI)-related pneumonia could cause significant morbidity, with possible discontinuation of therapy and possible mortality [118]. The time to onset of pneumonia ranges from 9 days to over 19 months after the initiation of therapy, with a median time of 2.8 months [118]. Imaging plays a crucial role in this effect detection. Although X-ray may be an initial tool, CT is able to detect all subtle changes in pneumonitis and help to differentiate among subtypes, as described by Delaunay et al. [122]. Investigations described 64 cases of pneumonia with the following CT patterns: (a) organized pneumonia (OP) (23%), (b) hypersensitivity pneumonitis (HP) (16%), (c) non-specific interstitial pneumonia (NSIP) (8%) and (d) bronchiolitis (6%). Some patients were diagnosed with concomitant patterns and a distinctive pattern was not identified in 36% of cases [122]. OP's pattern usually shows bilateral peribronchovascular and subpleural ground-glass and airspace opacities, with mid- to lower-lung predominance (Figure 2).

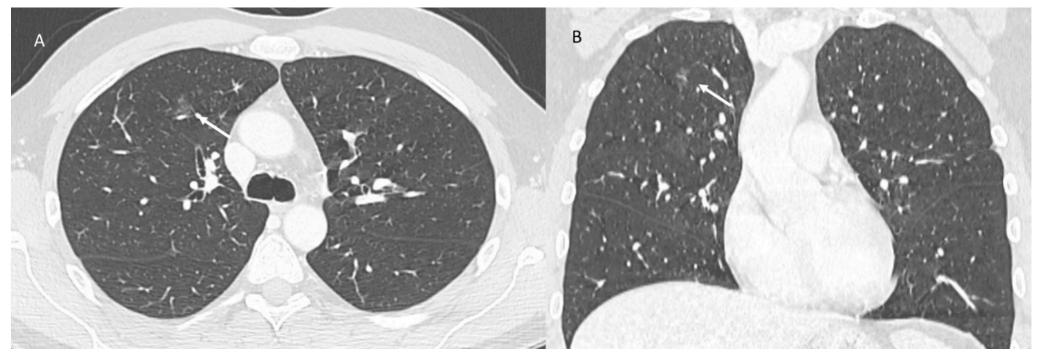


**Figure 2.** ICI-related pneumonitis. OP pattern on CT (axial: (A) and coronal: (B)): ground-glass and airspace opacities (arrows).

In addition, an inverted halo or atoll sign is detected. Pulmonary nodules, usually with peribronchovascular distribution and generally smaller (<10 mm) nodules, may also be detected. However, in some cases, the nodules may be nodular and massive with pointed edges, mimicking findings of malignancy [118,122]. These features should be distinguished from progression of malignancy (concurrent worsening of disease in other areas) and infection (clinical history, laboratory findings, response to appropriate therapy).

The NSIP pattern commonly manifests as ground glass and lattice opacities predominantly in the lower lobe. Airspace disease is temporally homogeneous and relatively symmetrical, with uncommon consolidation opacities, allowing NSIP patterns to be distinguished from OP patterns. Subpleural sparing of the posterior and inferior lobes has also been described as a specific feature. NSIP pattern should be distinguished from NSIP associated with autoimmune or connective tissue disease (appropriate medical history and condition-specific markers, no temporal relationship to immunotherapy course) and infection (clinical history, laboratory findings, response to appropriate therapy).

The HP pattern is associated with lower-grade symptoms. CT findings include diffuse or predominant ground-glass centrilobular nodules in the upper lobe, which may be related to air entrapment. This pattern should be distinguished from exposure-related HP (exposure and occupational history, no temporal relationship to immunotherapy course),

and from respiratory and follicular bronchiolitis (smoking history or underlying connective tissue and/or autoimmune disease history) and atypical infection (clinical history, laboratory findings, response to appropriate therapy).

Acute interstitial pneumonia (AIP)–acute respiratory distress syndrome (ARDS) is not a model of ICI therapy-related pneumonia, although it is associated with a more severe clinical course and extensive pulmonary involvement with imaging. This pattern is characterized by geographic or diffuse ground-glass or consolidation opacities involving most, and sometimes all, of the lungs, although lobular sparing areas may be detected. There may also be a thickening of the interlobular septum and a “crazy pavement” pattern (Figure 3). The differential diagnosis is extensive and includes pulmonary oedema, haemorrhage, and infection. The findings of ARDS may also be due to extrapulmonary causes such as pancreatitis, sepsis and/or shock and transfusion reactions.

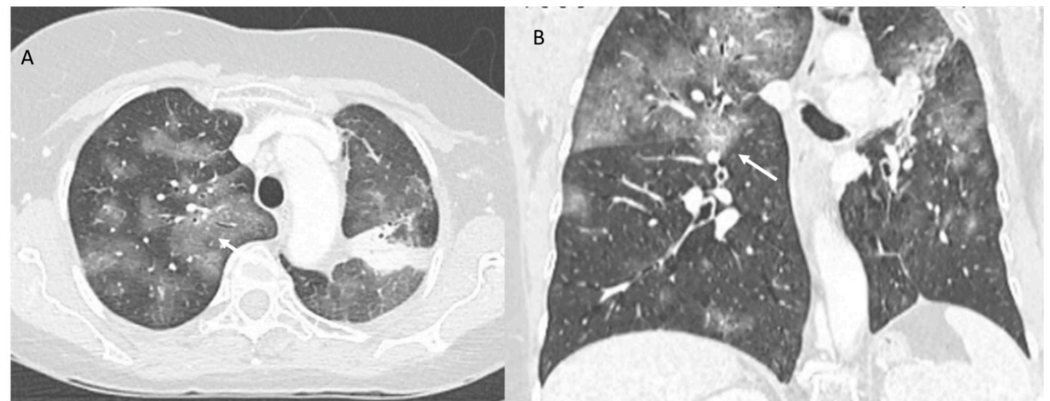


**Figure 3.** ICI-related pneumonitis. AIP-ARDS pattern on CT (axial: (A) and coronal: (B)): diffuse ground-glass opacities involving a majority of the lungs (arrows), although areas of lobular sparing can be detected.

The bronchiolitis pattern appears as a region of centrilobular nodularity, often seen in a tree-in-bud pattern. Thickening of the adjacent bronchial wall is frequently observed, as well as focal ground-glass and consolidation opacity, although this should not be the main feature. This pattern should be distinguished from aspiration (dependent lungs, airway and oesophageal secretion) and infection (clinical history, laboratory findings, response to appropriate therapy).

### 2.1. COVID-19 Vaccine Radiation Recall

Radiation recall reaction (RRR) is an infrequent but well-known event to clinicians, characterized by a late-occurring acute inflammatory reaction that develops in confined areas corresponding to previously irradiated radiation therapy (RT) treatment fields. RRR has been known to be triggered by a number of chemotherapy agents [123–132], including, recently, even COVID-19 vaccines [45]. It occurs in a variety of tissues, the commonest being skin, which accounts for two-thirds of reported cases. It is usually mild and self-limiting when the trigger drug is stopped. Re-challenge with the drug does not necessarily cause reactivation of the reaction.

This event has been reported within the lungs [52,118,133], determining radiation recall pneumonitis as acute inflammation within a previously irradiated area. The mechanism of the disease is unclear, but it seems to be related to an immune response. COVID-19 infection is known to cause immunological reactions, such as cytokine storm or multisystem inflammatory syndrome, in children [134–137]. Just like real infection, the developed vaccines are expected to induce an immune response. The inflammatory state created by the vaccine can favour the development of radiation recall. In fact, the few available papers on the topic suggest that COVID-19 vaccine can cause RRR, considering the time of vaccine administration and this event (Figure 4) [52,133]. The radioactive recall pneumonia model

includes consolidated or ground-glass opacities. It should be suspected in all patients with previous radiotherapy with new airspace changes clearly demarcated from the adjacent lung. The main differential diagnosis is infection that does not respect boundaries and occurs outside of the previous radiation field.



**Figure 4.** Radiation recall pneumonitis (CT scan axial: (A) and coronal: (B)) pattern includes consolidative opacities limited (arrows) to a prior radiation field.

## 2.2. Pneumonitis COVID-19

Typical chest CT imaging findings for COVID-19 patients are ground-glass opacity with bilateral multifocal patches or consolidation with the interlobular septum and vascular thickening in peripheral areas of the lungs [134–142]. These manifestations may also be compatible with other viral pneumonias [143]. In this scenario, the current gold standard for diagnosing COVID-19 is based on a molecular reverse transcription polymerase chain reaction (RT-PCR) test, aimed at detecting virus RNA in respiratory samples such as nasopharynx swabs or bronchial aspirate [144].

Compared to RT-PCR, the specificity of CT in detecting COVID-19 is lower, with an overall reported specificity of 46–80% [145–147]. This is due to the fact that the typical pattern of COVID-19 pneumonia shows a partial overlap with that of other lung diseases: ground-glass opacity (GGO), consolidation, crazy pavement, and enlargement of subsegmental vessels (diameter greater than 3 mm) in the GGO areas [148–150]. The temporal course of these anomalies was described by Pan et al., reporting four phases of the disease: initial stage (0–4 days after the onset of symptoms) with GGO as the main finding (Figure 5), progressive stage (5–8 days after onset of symptoms) with widespread GGO, mad pattern and consolidation, peak stage (9–13 days after onset of symptoms) with consolidation becoming more prevalent (Figure 6) and advanced stage ( $\geq 14$  days after the onset of symptoms) with gradual absorption of anomalies (Figure 7) [151]. A recent study examined the performance of radiologists in differentiating COVID-19 from non-COVID-19 viral pneumonia, revealing an accuracy of between 60 and 83% [152].

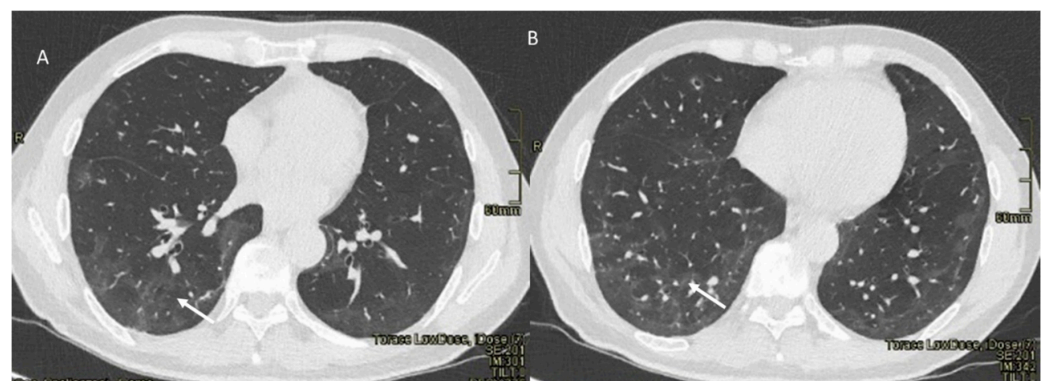


**Figure 5.** COVID-19 patient. CT (axial plane: (A,B)) shows early stage with GGO (arrow) as main finding.

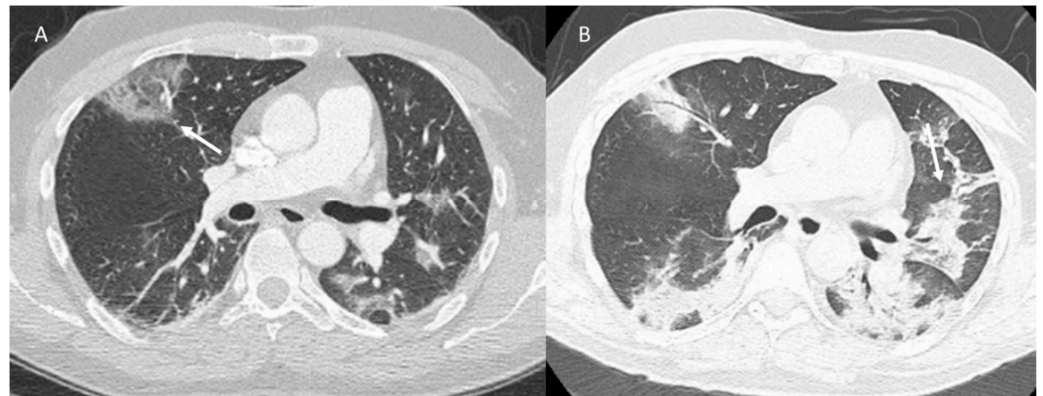


**Figure 6.** COVID-19 patient at peak stage. CT (axial plane: (A,B)) shows consolidation (arrow).



**Figure 7.** COVID-19 patient at late stage. CT (axial plane: (A,B)) shows fibrotic-like changes (arrow).

COVID-19 pneumonia may be misdiagnosed as non-COVID-19 lung disease in the early and late stages, reflecting the fact that the typical early-stage pattern and the absorption of late features are commonly linked to signs of organizational pneumonia or signs of early fibrosis. These characteristics can be found in different conditions and, therefore, this aspect should be considered non-specific [148–152].

### 3. Discussion

Since the population continues to be infected or vaccinated in larger numbers, COVID-19 pneumonitis and RRR pneumonitis caused by COVID-19 vaccination will be increasingly seen by radiologists and could result in imaging test call-backs, additional workups, and false-positive results. In addition, considering oncological patients who could develop drug-related pneumonitis or a pattern of PLC as a progressive disease, it is clear as these conditions should be taken into account for a correct diagnosis. Therefore, a correct medical history is essential to ruling out the possibility of a recent infection as well as recent vaccine administration.

RRR and SARS-CoV-2 interstitial pneumonia, so non-COVID-19-related pneumonia, show overlapping clinical features. In fact, the most common symptoms are dyspnoea and dry non-productive cough and fever. Additionally, chest CT findings are also very similar, as the radiological characteristics of COVID-19 and non-COVID-19-related pneumonia are GGO in the initial phase, patchy areas of consolidation in the peak phase and fibrotic changes in the dissipative phase [8,14].

Where the cause of the lung abnormalities is unclear, due to radiological CT findings being unspecific, multidisciplinary management would be correct to establish the main proper treatment. Although the management of oncological patients should consider the probability of malignant lung involvement with disease progression or adverse effects of

specific therapies, it is clear that in pandemic conditions, several unspecific features may be related to an undiagnosed infection. Although the typical pattern of COVID-19 pneumonitis should be identified with high accuracy in symptomatic patients, this could be complicated if infection has been not diagnosed, especially in the post-infection phase. Therefore, we should consider several features, such as that the typical RRR pattern is usually strictly related to the target volume and to the dose distribution of the treatment plan, while during COVID-19 infection, the parenchymal involvement is not limited to a single lobe, although this is possible during the first phase. Additionally, PLC and ICI-related pneumonitis show diffuse parenchymal involvement. Additionally, in PLC, we find an irregularly interlobular septal thickening or nodular thickening, while in COVID-19 pneumonitis and RRR, septal thickening is more regular. These differences in chest CT patterns are the main factors that should help lead to a proper diagnosis (Table 1). However, distinguishing COVID-19 lung involvement or vaccine RRR from other lung pathologies such as cancer on chest CT may be straightforward, differentiation between COVID-19 and other pneumonias can be particularly troublesome for physicians because of the radiographic similarities, and this is particularly evident during the early or late phases of these pathologies. Inaccurate imaging interpretation makes it harder for patient management strategies to work efficiently.

**Table 1.** Lung involvement and CT pattern for pneumonia type.

Type of Pneumonia	Lung Involvement	CT-Patter
COVID-19 Pneumonia	Diffuse (related to the phase of disease)	ground-glass opacity, crazy-paving pattern, consolidative opacities, interlobular septal thickening (according to the phase of disease)
RRR-Related Vaccine	Target Area	Consolidative opacities
Pulmonary lymphangitis carcinomatosa	Diffuse (related to the phase of disease)	Irregularly interlobular septal thickening, smooth (early stage), or nodular thickening (late development), ground-glass opacity, pleural effusions.
ICI-Related Pneumonitis	Diffuse (related to the phase of disease)	ground-glass and reticular opacities, consolidative opacities, interlobular septal thickening, “crazy-paving” pattern

Interestingly, COVID-19 pneumonia and ICI-related pneumonitis have been suggested to share critical biological mechanisms, including the hyperactivation of immune cells associated with a significant increase in pro-inflammatory cytokines. Distinguishing between COVID-19 pneumonia and ICI-related pneumonitis is a diagnostic challenge. ICI-related pneumonitis might present with several patterns. These patterns seemingly overlap the CT features of COVID-19 pneumonia, possibly due to overlapped biological mechanisms.

Recently, the progressive integration of radiomics approaches and artificial intelligence (AI)-based solutions could be of help. To date, the application of AI in medical imaging has improved the assessment and early diagnosis of neurodegenerative diseases and heart disease, with a particularly high impact on breast and lung cancer [153–162]. A cutting-edge research direction leverages deep learning (DL) and machine learning (ML) to understand COVID-19. AI could be used for the detection and quantification of COVID-19 disease from X-ray and CT images [163–165], enabling correct patient diagnosis and management. Deep learning (DL), a form of AI, has been successfully applied to chest CT imaging to distinguish COVID-19 pneumonia from community-acquired infections, as well as to provide qualitative and quantitative analyses for disease burden estimation and facilitating and expediting imaging interpretation [166]. However, deep learning algorithms based only on CT images cannot distinguish COVID-19 pneumonia from other lung interstitial diseases with overlapping CT features with high specificity; thus, adding clinical/laboratory findings to the algorithm can improve the diagnostic performance based on binary classification [167,168].

#### 4. Conclusions

Knowing the chest imaging features related to COVID-19 infection or vaccine is critical to avoid misleading results in patients and clinicians and determine the idea of a disease progression or an adverse treatment effect. In this context, we should consider several features, as the typical RRR pattern is usually strictly related to the target volume and the dose distribution of the treatment plan. At the same time, during COVID-19 infection, parenchymal involvement is not limited to a single lobe, although this is possible during the first phase. Additionally, PLC and ICI-related pneumonitis show a diffuse parenchymal involvement. The PLC shows an irregularly interlobular septal thickening or nodular thickening, while septal thickening is common in COVID-19 pneumonitis and RRR. These differences in chest CT patterns are the main factors that should help for proper diagnosis. However, distinguishing COVID-19 lung involvement or vaccine RRR from other lung pathologies on chest CT may be straightforward, particularly during the early or late phases of these pathologies.

**Author Contributions:** Conceptualization, S.I., V.M. and V.G.; Investigation, R.F., I.S., A.V., F.G., F.D., R.G., D.C., E.B., P.P., A.B. (Alessandra Borgheresi), A.G., A.B. (Antonio Barile) and V.G.; Methodology, R.F., I.S., A.V., F.G., F.D., R.G., D.C., E.B., P.P., A.B. (Alessandra Borgheresi), A.G., V.M., A.B. (Alessandra Borgheresi) and V.G. Each author has participated sufficiently to take public responsibility for the content of the manuscript. All authors have read and agreed to the published version of the manuscript.

**Funding:** This research received no external funding.

**Institutional Review Board Statement:** The study was conducted according to the guidelines of the Declaration of Helsinki. Approval by the Institutional Review Board was not needed considering the nature of the study: the findings are a description of a single case report.

**Informed Consent Statement:** Informed consent was obtained from the patient.

**Data Availability Statement:** Data are available at <https://zenodo.org/record/6393020#.YkgKd-hBy3A> (accessed on 21 January 2022).

**Acknowledgments:** The authors are grateful to Alessandra Trocino, librarian at the National Cancer Institute of Naples, Italy. Moreover, for their collaboration, the authors are grateful for the research support of Paolo Pariante, Martina Totaro and Andrea Esposito of Radiology Division, “Istituto Nazionale Tumori IRCCS Fondazione Pascale—IRCCS di Napoli”, Naples, I-80131, Italy.

**Conflicts of Interest:** The authors have no conflict of interest to disclose.

#### References

1. Stramare, R.; Carretta, G.; Capizzi, A.; Boemo, D.G.; Contessa, C.; Motta, R.; De Conti, G.; Causin, F.; Giraud, C.; Donato, D. Radiological management of COVID-19: Structure your diagnostic path to guarantee a safe path. *Radiol. Med.* **2020**, *125*, 691–694. [[CrossRef](#)] [[PubMed](#)]
2. Granata, V.; Fusco, R.; Izzo, F.; Setola, S.V.; Coppola, M.; Grassi, R.; Reginelli, A.; Cappabianca, S.; Petrillo, A. COVID-19 infection in cancer patients: The management in a diagnostic unit. *Radiol. Oncol.* **2021**, *55*, 121–129. [[CrossRef](#)] [[PubMed](#)]
3. Gaia, C.; Chiara, C.M.; Silvia, L.; Chiara, A.; Luisa, D.C.M.; Giulia, B.; Silvia, P.; Lucia, C.; Alessandra, T.; Annarita, S.; et al. Chest CT for early detection and management of coronavirus disease (COVID-19): A report of 314 patients admitted to Emergency Department with suspected pneumonia. *Radiol. Med.* **2020**, *125*, 931–942. [[CrossRef](#)] [[PubMed](#)]
4. Gabelloni, M.; Faggioni, L.; Cioni, D.; Mendola, V.; Falaschi, Z.; Coppola, S.; Corradi, F.; Isirdi, A.; Brandi, N.; Coppola, F.; et al. Extracorporeal membrane oxygenation (ECMO) in COVID-19 patients: A pocket guide for radiologists. *Radiol. Med.* **2022**, *13*, 369–382. [[CrossRef](#)] [[PubMed](#)]
5. Giovagnoni, A. Facing the COVID-19 emergency: We can, and we do. *Radiol. Med.* **2020**, *125*, 337–338. [[CrossRef](#)]
6. Montesi, G.; Di Biase, S.; Chierchini, S.; Pavanato, G.; Viridis, G.E.; Contato, E.; Mandoliti, G. Radiotherapy during COVID-19 pandemic. How to create a No fly zone: A Northern Italy experience. *Radiol. Med.* **2020**, *125*, 600–603. [[CrossRef](#)]
7. Ierardi, A.M.; Wood, B.J.; Arrichiello, A.; Bottino, N.; Bracchi, L.; Forzenigo, L.; Andrisani, M.C.; Vespro, V.; Bonelli, C.; Amalou, A.; et al. Preparation of a radiology department in an Italian hospital dedicated to COVID-19 patients. *Radiol. Med.* **2020**, *125*, 894–901. [[CrossRef](#)]

8. Grassi, R.; Cappabianca, S.; Urraro, F.; Feragalli, B.; Montanelli, A.; Patelli, G.; Granata, V.; Giacobbe, G.; Russo, G.M.; Grillo, A.; et al. Chest CT Computerized Aided Quantification of PNEUMONIA Lesions in COVID-19 Infection: A Comparison among Three Commercial Software. *Int. J. Environ. Res. Public Health* **2020**, *17*, 6914. [[CrossRef](#)]
9. Pediconi, F.; Galati, F.; Bernardi, D.; Belli, P.; Brancato, B.; Calabrese, M.; Camera, L.; Carbonaro, L.A.; Caumo, F.; Clauser, P.; et al. Breast imaging and cancer diagnosis during the COVID-19 pandemic: Recommendations from the Italian College of Breast Radiologists by SIRM. *Radiol. Med.* **2020**, *125*, 926–930. [[CrossRef](#)]
10. Koç, A.; Sezgin, S.; Kayipmaz, S. Comparing different planimetric methods on volumetric estimations by using cone beam computed tomography. *Radiol. Med.* **2020**, *125*, 398–405. [[CrossRef](#)]
11. WHO Coronavirus (COVID-19) Dashboard. Available online: <https://covid19.who.int> (accessed on 21 January 2022).
12. Xu, X.W.; Wu, X.X.; Jiang, X.G.; Xu, K.J.; Ying, L.J.; Ma, C.L.; Li, S.B.; Wang, H.Y.; Zhang, S.; Gaon, H.N.; et al. Clinical findings in a group of patients infected with the 2019 novel coronavirus (SARS-CoV-2) outside of Wuhan, China: Retrospective case series. *BMJ* **2020**, *368*, m606. [[CrossRef](#)] [[PubMed](#)]
13. Chen, N.; Zhou, M.; Dong, X.; Qu, J.; Gong, F.; Han, Y.; Qui, Y.; Wang, J.; Liu, Y.; Wei, Y.; et al. Epidemiological and clinical characteristics of 99 cases of 2019 novel coronavirus pneumonia in Wuhan, China: A descriptive study. *Lancet* **2020**, *395*, 507–513. [[CrossRef](#)]
14. Wu, Z.; McGoogan, J.M. Characteristics of and important lessons from the coronavirus disease 2019 (COVID-19) outbreak in China: Summary of a report of 72 314 cases from the Chinese center for disease control and prevention. *JAMA* **2020**, *323*, 1239–1242. [[CrossRef](#)] [[PubMed](#)]
15. Han, C.; Duan, C.; Zhang, S.; Spiegel, B.; Shi, H.; Wang, W.; Zhang, L.; Lin, R.; Liu, J.; Ding, Z.; et al. Digestive Symptoms in COVID-19 Patients with Mild Disease Severity: Clinical Presentation, Stool Viral RNA Testing, and Outcomes. *Am. J. Gastroenterol.* **2020**, *115*, 916–923. [[CrossRef](#)] [[PubMed](#)]
16. Pan, L.; Mu, M.; Yang, P.; Sun, Y.; Wang, R.; Yan, J.; Li, P.; Hu, B.; Wang, J.; Hu, C.; et al. Clinical characteristics of COVID-19 patients with digestive symptoms in Hubei, China: A descriptive, cross-sectional, multicenter study. *Am. J. Gastroenterol.* **2020**, *115*, 766–773. [[CrossRef](#)] [[PubMed](#)]
17. Liu, W.; Zhang, Q.; Chen, J.; Xiang, R.; Song, H.; Shu, S.; Chen, L.; Liang, L.; Zhou, J.; You, L.; et al. Detection of COVID-19 in children in early January 2020 in Wuhan, China. *N. Engl. J. Med.* **2020**, *382*, 1370–1371. [[CrossRef](#)]
18. Lu, X.; Zhang, L.; Du, H.; Zhang, J.; Li, Y.Y.; Qu, J.; Zhang, W.; Wang, Y.; Bao, S.; Li, Y.; et al. SARS-CoV-2 Infection in Children. *N. Engl. J. Med.* **2020**, *382*, 1663–1665. [[CrossRef](#)]
19. Hu, Z.; Song, C.; Xu, C.; Jin, G.; Chen, Y.; Xu, X.; Ma, X.; Chen, W.; Lin, Y.; Zheng, Y.; et al. Clinical characteristics of 24 asymptomatic infections with COVID-19 screened among close contacts in Nanjing, China. *Sci. China Life Sci.* **2020**, *63*, 706–711. [[CrossRef](#)]
20. Wang, Y.; Liu, Y.; Liu, L.; Wang, X.; Luo, N.; Li, L. Clinical Outcomes in 55 Patients with Severe Acute Respiratory Syndrome Coronavirus 2 Who Were Asymptomatic at Hospital Admission in Shenzhen, China. *J. Infect. Dis.* **2020**, *221*, 1770–1774. [[CrossRef](#)]
21. Mizumoto, K.; Kagaya, K.; Zarebski, A.; Chowell, G. Estimating the asymptomatic proportion of coronavirus disease 2019 (COVID-19) cases on board the Diamond Princess cruise ship, Yokohama, Japan, 2020. *Euro Surveill.* **2020**, *25*, 2000180. [[CrossRef](#)]
22. Pan, X.; Chen, D.; Xia, Y.; Wu, X.; Li, T.; Ou, X.; Zhou, L.; Liu, J. Asymptomatic cases in a family cluster with SARS-CoV-2 infection. *Lancet Infect Dis.* **2020**, *20*, 410–411. [[CrossRef](#)]
23. Agostini, A.; Floridi, C.; Borgheresi, A.; Badaloni, M.; Pirani, P.E.; Terilli, F.; Ottaviani, L.; Giovagnoni, A. Proposal of a low-dose, long-pitch, dual-source chest CT protocol on third-generation dual-source CT using a tin filter for spectral shaping at 100 kVp for Coronavirus Disease 2019 (COVID-19) patients: A feasibility study. *Radiol. Med.* **2020**, *125*, 365–373. [[CrossRef](#)] [[PubMed](#)]
24. Borghesi, A.; Maroldi, R. COVID-19 outbreak in Italy: Experimental chest X-ray scoring system for quantifying and monitoring disease progression. *Radiol. Med.* **2020**, *125*, 509–513. [[CrossRef](#)] [[PubMed](#)]
25. Neri, E.; Miele, V.; Coppola, F.; Grassi, R. Use of CT and artificial intelligence in suspected or COVID-19 positive patients: Statement of the Italian Society of Medical and Interventional Radiology. *Radiol. Med.* **2020**, *125*, 505–508. [[CrossRef](#)]
26. Carotti, M.; Salaffi, F.; Sarzi-Puttini, P.; Agostini, A.; Borgheresi, A.; Minorati, D.; Galli, M.; Marotto, D.; Giovagnoni, A. Chest CT features of coronavirus disease 2019 (COVID-19) pneumonia: Key points for radiologists. *Radiol. Med.* **2020**, *125*, 636–646. [[CrossRef](#)]
27. Fusco, R.; Grassi, R.; Granata, V.; Setola, S.V.; Grassi, F.; Cozzi, D.; Pecori, B.; Izzo, F.; Petrillo, A. Artificial Intelligence and COVID-19 Using Chest CT Scan and Chest X-ray Images: Machine Learning and Deep Learning Approaches for Diagnosis and Treatment. *J. Pers. Med.* **2021**, *11*, 993. [[CrossRef](#)] [[PubMed](#)]
28. Borghesi, A.; Zigliani, A.; Masciullo, R.; Golemi, S.; Maculotti, P.; Farina, D.; Maroldi, R. Radiographic severity index in COVID-19 pneumonia: Relationship to age and sex in 783 Italian patients. *Radiol. Med.* **2020**, *125*, 461–464. [[CrossRef](#)]
29. Cozzi, D.; Albanesi, M.; Cavigli, E.; Moroni, C.; Bindi, A.; Luvarà, S.; Lucarini, S.; Busoni, S.; Mazzoni, L.N.; Miele, V. Chest X-ray in new Coronavirus Disease 2019 (COVID-19) infection: Findings and correlation with clinical outcome. *Radiol. Med.* **2020**, *125*, 730–737. [[CrossRef](#)]
30. Gatti, M.; Calandri, M.; Barba, M.; Biondo, A.; Geninatti, C.; Gentile, S.; Greco, M.; Morrone, V.; Piatti, C.; Santonocito, A.; et al. Baseline chest X-ray in coronavirus disease 19 (COVID-19) patients: Association with clinical and laboratory data. *Radiol. Med.* **2020**, *125*, 1271–1279. [[CrossRef](#)]

31. Giannitto, C.; Sposta, F.M.; Repici, A.; Vatteroni, G.; Casiraghi, E.; Casari, E.; Ferraroli, G.M.; Fugazza, A.; Sandri, M.T.; Chiti, A.; et al. Chest CT in patients with a moderate or high pretest probability of COVID-19 and negative swab. *Radiol. Med.* **2020**, *125*, 1260–1270. [[CrossRef](#)]
32. Machitori, A.; Noguchi, T.; Kawata, Y.; Horioka, N.; Nishie, A.; Kakihara, D.; Ishigami, K.; Aoki, S.; Imai, Y. Computed tomography surveillance helps tracking COVID-19 outbreak. *Jpn. J. Radiol.* **2020**, *38*, 1169–1176. [[CrossRef](#)] [[PubMed](#)]
33. Available online: <https://www.aifa.gov.it> (accessed on 21 January 2022).
34. Granata, V.; Fusco, R.; Setola, S.V.; Galdiero, R.; Picone, C.; Izzo, F.; D’Aniello, R.; Miele, V.; Grassi, R.; Grassi, R.; et al. Lymphadenopathy after BNT162b2 COVID-19 Vaccine: Preliminary Ultrasound Findings. *Biology* **2021**, *10*, 214. [[CrossRef](#)] [[PubMed](#)]
35. Moderna COVID-19 Vaccine. 2021. Available online: <https://www.fda.gov/emergency-preparedness-and-response/coronavirus-disease-2019-covid-19/moderna-covid-19-vaccine> (accessed on 8 April 2021).
36. Pfizer-BioNTech COVID-19 Vaccine. 2021. Available online: <https://www.fda.gov/emergency-preparedness-and-response/coronavirus-disease-2019-covid-19/pfizer-biontech-covid-19-vaccine> (accessed on 21 January 2022).
37. Janssen COVID-19 Vaccine. 2021. Available online: <https://www.fda.gov/emergency-preparedness-and-response/coronavirus-disease-2019-covid-19/janssen-covid-19-vaccine> (accessed on 21 January 2022).
38. Baden, L.R.; El Sahly, H.M.; Essink, B.; Kotloff, K.; Frey, S.; Novak, R.; Diemert, D.; Spector, S.A.; Rouphael, N.; Creech, C.B.; et al. Efficacy and safety of the mRNA-1273 SARS-CoV-2 vaccine. *N. Engl. J. Med.* **2021**, *384*, 403–416. [[CrossRef](#)] [[PubMed](#)]
39. Polack, F.P.; Thomas, S.J.; Kitchin, N.; Absalon, J.; Gurtman, A.; Lockhart, S.; Perez, J.L.; Pérez Marc, G.; Moreira, E.D.; Zerbini, C.; et al. Safety and efficacy of the BNT162b2 mRNA COVID-19 Vaccine. *N. Engl. J. Med.* **2020**, *383*, 2603–2615. [[CrossRef](#)]
40. Local Reactions, Systemic Reactions, Adverse Events, and Serious Adverse Events: Pfizer-BioNTech COVID-19 Vaccine. 2021. Available online: <https://www.cdc.gov/vaccines/covid-19/info-by-product/pfizer/reactogenicity.html> (accessed on 4 August 2021).
41. Di Serafino, M.; Notaro, M.; Rea, G.; Iacobellis, F.; Paoli, V.D.; Acampora, C.; Ianniello, S.; Brunese, L.; Romano, L.; Vallone, G. The lung ultrasound: Facts or artifacts? In the era of COVID-19 outbreak. *Radiol. Med.* **2020**, *125*, 738–753. [[CrossRef](#)]
42. Reginelli, A.; Grassi, R.; Feragalli, B.; Belfiore, M.; Montanelli, A.; Patelli, G.; La Porta, M.; Urraro, F.; Fusco, R.; Granata, V.; et al. Coronavirus Disease 2019 (COVID-19) in Italy: Double Reading of Chest CT Examination. *Biology* **2021**, *10*, 89. [[CrossRef](#)]
43. Grassi, R.; Belfiore, M.P.; Montanelli, A.; Patelli, G.; Urraro, F.; Giacobbe, G.; Fusco, R.; Granata, V.; Petrillo, A.; Sacco, P.; et al. COVID-19 pneumonia: Computer-aided quantification of healthy lung parenchyma, emphysema, ground glass and consolidation on chest computed tomography (CT). *Radiol. Med.* **2020**, *126*, 553–560. [[CrossRef](#)]
44. Özel, M.; Aslan, A.; Araç, S. Use of the COVID-19 Reporting and Data System (CO-RADS) classification and chest computed tomography involvement score (CT-IS) in COVID-19 pneumonia. *Radiol. Med.* **2021**, *126*, 679–687. [[CrossRef](#)]
45. Soyfer, V.; Gutfeld, O.; Shamai, S.; Schlocker, A.; Merimsky, O. COVID-19 Vaccine-Induced Radiation Recall Phenomenon. *Int. J. Radiat. Oncol.* **2021**, *110*, 957–961. [[CrossRef](#)]
46. Marples, R.; Douglas, C.; Xavier, J.; Collins, A.-J. Breast Radiation Recall Phenomenon After Astra-Zeneca COVID-19 Vaccine: A Case Series. *Cureus* **2022**, *14*, e21499. [[CrossRef](#)]
47. Ishikawa, Y.; Umezawa, R.; Yamamoto, T.; Takahashi, N.; Takeda, K.; Suzuki, Y.; Jingu, K. Radiation recall phenomenon after administration of the mRNA-1273 SARS-CoV-2 vaccine. *Int. Cancer Conf. J.* **2022**, *11*, 91–95. [[CrossRef](#)] [[PubMed](#)]
48. Shinada, K.; Murakami, S.; Yoshida, D.; Saito, H. Radiation recall pneumonitis after COVID-19 vaccination. *Thorac. Cancer* **2021**, *13*, 144–145. [[CrossRef](#)]
49. Ierardi, A.M.; Gaibazzi, N.; Tuttolomondo, D.; Fusco, S.; La Mura, V.; Peyvandi, F.; Aliberti, S.; Blasi, F.; Cozzi, D.; Carrafiello, G.; et al. Deep vein thrombosis in COVID-19 patients in general wards: Prevalence and association with clinical and laboratory variables. *Radiol. Med.* **2021**, *126*, 722–728. [[CrossRef](#)] [[PubMed](#)]
50. Ippolito, D.; Giandola, T.; Maino, C.; Pecorelli, A.; Capodaglio, C.; Ragusi, M.; Porta, M.; Gandola, D.; Masetto, A.; Drago, S.; et al. Acute pulmonary embolism in hospitalized patients with SARS-CoV-2-related pneumonia: Multicentric experience from Italian endemic area. *Radiol. Med.* **2021**, *126*, 669–678. [[CrossRef](#)] [[PubMed](#)]
51. Hughes, N.M.; Hammer, M.M.; Awad, M.M.; Jacene, H.A. Radiation Recall Pneumonitis on FDG PET/CT Triggered by COVID-19 Vaccination. *Clin. Nucl. Med.* **2021**, *47*, e281–e283. [[CrossRef](#)] [[PubMed](#)]
52. Steber, C.R.; Ponnatapura, J.; Hughes, R.T.; Farris, M.K. Rapid Development of Clinically Symptomatic Radiation Recall Pneumonitis Immediately Following COVID-19 Vaccination. *Cureus* **2021**, *13*, e14303. [[CrossRef](#)]
53. Moroni, C.; Cozzi, D.; Albanesi, M.; Cavigli, E.; Bindi, A.; Luvarà, S.; Busoni, S.; Mazzoni, L.N.; Grifoni, S.; Nazerian, P.; et al. Chest X-ray in the emergency department during COVID-19 pandemic descending phase in Italy: Correlation with patients’ outcome. *Radiol. Med.* **2021**, *126*, 661–668. [[CrossRef](#)]
54. Cereser, L.; Girometti, R.; Da Re, J.; Marchesini, F.; Como, G.; Zuiani, C. Inter-reader agreement of high-resolution computed tomography findings in patients with COVID-19 pneumonia: A multi-reader study. *Radiol. Med.* **2021**, *126*, 577–584. [[CrossRef](#)]
55. McKay, M.J.; Foster, R. Radiation recall reactions: An oncologic enigma. *Crit. Rev. Oncol.* **2021**, *168*, 103527. [[CrossRef](#)]
56. Klimek, M. Pulmonary lymphangitis carcinomatosa: Systematic review and meta-analysis of case reports, 1970–2018. *Postgrad. Med.* **2019**, *131*, 309–318. [[CrossRef](#)]
57. Kumar, A.K.; Mantri, S.N. *Lymphangitic Carcinomatosis*; StatPearls Publishing: Treasure Island, FL, USA, 2021. Available online: <https://www.ncbi.nlm.nih.gov/books/NBK560921/> (accessed on 21 January 2022).

58. Lin, W.-R.; Lai, R.-S. Pulmonary lymphangitic carcinomatosis. *QJM* **2014**, *107*, 935–936. [[CrossRef](#)] [[PubMed](#)]
59. Liguori, C.; Farina, D.; Vaccher, F.; Ferrandino, G.; Bellini, D.; Carbone, I. Myocarditis: Imaging up to date. *Radiol. Med.* **2020**, *125*, 1124–1134. [[CrossRef](#)] [[PubMed](#)]
60. Shaw, B.; Daskareh, M.; Gholamrezanezhad, A. The lingering manifestations of COVID-19 during and after convalescence: Update on long-term pulmonary consequences of coronavirus disease 2019 (COVID-19). *Radiol. Med.* **2021**, *126*, 40–46. [[CrossRef](#)] [[PubMed](#)]
61. Rawashdeh, M.A.; Saade, C. Radiation dose reduction considerations and imaging patterns of ground glass opacities in coronavirus: Risk of over exposure in computed tomography. *Radiol. Med.* **2021**, *126*, 380–387. [[CrossRef](#)] [[PubMed](#)]
62. Gomatou, G.; Tzilas, V.; Kotteas, E.; Syrigos, K.; Bouros, D. Immune Checkpoint Inhibitor-Related Pneumonitis. *Respiration* **2020**, *99*, 932–942. [[CrossRef](#)]
63. Naidoo, J.; Wang, X.; Woo, K.M.; Iyriboz, T.; Halpenny, D.; Cunningham, J.; Chaft, J.E.; Segal, N.H.; Callahan, M.K.; Lesokhin, A.M.; et al. Pneumonitis in Patients Treated With Anti-Programmed Death-1/Programmed Death Ligand 1 Therapy. *J. Clin. Oncol.* **2017**, *35*, 709–717. [[CrossRef](#)]
64. Suresh, K.; Naidoo, J.; Lin, C.T.; Danoff, S. Immune Checkpoint Immunotherapy for Non-Small Cell Lung Cancer: Benefits and Pulmonary Toxicities. *Chest* **2018**, *154*, 1416–1423. [[CrossRef](#)]
65. Zhong, L.; Altan, M.; Shannon, V.R.; Sheshadri, A. Immune-Related Adverse Events: Pneumonitis. *Adv. Exp. Med. Biol.* **2020**, *1244*, 255–269. [[CrossRef](#)]
66. Lombardi, A.F.; Afsahi, A.M.; Gupta, A.; Gholamrezanezhad, A. Severe acute respiratory syndrome (SARS), Middle East respiratory syndrome (MERS), influenza, and COVID-19, beyond the lungs: A review article. *Radiol. Med.* **2021**, *126*, 561–569. [[CrossRef](#)]
67. Cozzi, D.; Bindi, A.; Cavigli, E.; Grosso, A.M.; Luvarà, S.; Morelli, N.; Moroni, C.; Piperio, R.; Miele, V.; Bartolucci, M. Exogenous lipoid pneumonia: When radiologist makes the difference. *Radiol. Med.* **2021**, *126*, 22–28. [[CrossRef](#)]
68. Palmisano, A.; Scotti, G.M.; Ippolito, D.; Morelli, M.J.; Vignale, D.; Gandola, D.; Sironi, S.; De Cobelli, F.; Ferrante, L.; Spessot, M.; et al. Chest CT in the emergency department for suspected COVID-19 pneumonia. *Radiol. Med.* **2021**, *126*, 498–502. [[CrossRef](#)] [[PubMed](#)]
69. Jain, A.; Shannon, V.R.; Sheshadri, A. Immune-Related Adverse Events: Pneumonitis. *Immunotherapy* **2018**, *995*, 131–149. [[CrossRef](#)]
70. Suresh, K.; Naidoo, J.; Zhong, Q.; Xiong, Y.; Mammen, J.; De Flores, M.V.; Cappelli, L.; Balaji, A.; Palmer, T.; Forde, P.M.; et al. The alveolar immune cell landscape is dysregulated in checkpoint inhibitor pneumonitis. *J. Clin. Investig.* **2019**, *129*, 4305–4315. [[CrossRef](#)] [[PubMed](#)]
71. Bruce, D.M.; Heys, S.D.; Eremin, O. Lymphangitis carcinomatosa: A literature review. *J. R. Coll. Surg. Edinb.* **1996**, *41*, 7–13. [[PubMed](#)]
72. Kazawa, N.; Kitaichi, M.; Hiraoka, M.; Togashi, K.; Mio, N.; Mishima, M.; Wada, H. Small cell lung carcinoma: Eight types of extension and spread on computed tomography. *J. Comput. Assist. Tomogr.* **2006**, *30*, 653–661. [[CrossRef](#)] [[PubMed](#)]
73. Jiménez-Fonseca, P.; On behalf of the EPIPHANY study investigators and the Asociación de Investigación de la Enfermedad Tromboembólica de la Región de Murcia; Carmona-Bayonas, A.; Font, C.; Plasencia-Martínez, J.; Calvo-Temprano, D.; Otero, R.; Beato, C.; Biosca, M.; Sánchez, M.; et al. The prognostic impact of additional intrathoracic findings in patients with cancer-related pulmonary embolism. *Clin. Transl. Oncol.* **2018**, *20*, 230–242. [[CrossRef](#)]
74. Caruso, D.; Polici, M.; Zerunian, M.; Pucciarelli, F.; Polidori, T.; Guido, G.; Rucci, C.; Bracci, B.; Muscogiuri, E.; De Dominicis, C.; et al. Quantitative Chest CT analysis in discriminating COVID-19 from non-COVID-19 patients. *Radiol. Med.* **2020**, *126*, 243–249. [[CrossRef](#)] [[PubMed](#)]
75. Cardobi, N.; Benetti, G.; Cardano, G.; Arena, C.; Micheletto, C.; Cavedon, C.; Montemezzi, S. CT radiomic models to distinguish COVID-19 pneumonia from other interstitial pneumonias. *Radiol. Med.* **2021**, *126*, 1037–1043. [[CrossRef](#)]
76. Caruso, D.; Pucciarelli, F.; Zerunian, M.; Ganeshan, B.; De Santis, D.; Polici, M.; Rucci, C.; Polidori, T.; Guido, G.; Bracci, B.; et al. Chest CT texture-based radiomics analysis in differentiating COVID-19 from other interstitial pneumonia. *Radiol. Med.* **2021**, *126*, 1415–1424. [[CrossRef](#)]
77. Masselli, G.; Almerberger, M.; Tortora, A.; Capoccia, L.; Dolciami, M.; D’Aprile, M.R.; Valentini, C.; Avventurieri, G.; Bracci, S.; Ricci, P. Role of CT angiography in detecting acute pulmonary embolism associated with COVID-19 pneumonia. *Radiol. Med.* **2021**, *126*, 1553–1560. [[CrossRef](#)]
78. Pecoraro, M.; Cipollari, S.; Marchitelli, L.; Messina, E.; Del Monte, M.; Galea, N.; Ciardi, M.R.; Francone, M.; Catalano, C.; Panebianco, V. Cross-sectional analysis of follow-up chest MRI and chest CT scans in patients previously affected by COVID-19. *Radiol. Med.* **2021**, *126*, 1273–1281. [[CrossRef](#)] [[PubMed](#)]
79. Granata, V.; Ianniello, S.; Fusco, R.; Urraro, F.; Pupo, D.; Magliocchetti, S.; Albarello, F.; Campioni, P.; Cristofaro, M.; Di Stefano, F.; et al. Quantitative Analysis of Residual COVID-19 Lung CT Features: Consistency among Two Commercial Software. *J. Pers. Med.* **2021**, *11*, 1103. [[CrossRef](#)]
80. Granata, V.; Fusco, R.; Bicchierai, G.; Cozzi, D.; Grazzini, G.; Danti, G.; De Muzio, F.; Maggialelli, N.; Smorchkova, O.; D’Elia, M.; et al. Diagnostic protocols in oncology: Workup and treatment planning: Part 1: The optimization of CT protocol. *Eur. Rev. Med. Pharmacol. Sci.* **2021**, *25*, 6972–6994. [[PubMed](#)]

81. Rampado, O.; Depaoli, A.; Marchisio, F.; Gatti, M.; Racine, D.; Ruggeri, V.; Ruggirello, I.; Darvizeh, F.; Fonio, P.; Ropolo, R. Effects of different levels of CT iterative reconstruction on low-contrast detectability and radiation dose in patients of different sizes: An anthropomorphic phantom study. *Radiol. Med.* **2020**, *126*, 55–62. [[CrossRef](#)] [[PubMed](#)]
82. Schicchi, N.; Fogante, M.; Palumbo, P.; Agliata, G.; Pirani, P.E.; Di Cesare, E.; Giovagnoni, A. The sub-millisievert era in CTCA: The technical basis of the new radiation dose approach. *Radiol. Med.* **2020**, *125*, 1024–1039. [[CrossRef](#)]
83. Palumbo, P.; Cannizzaro, E.; Bruno, F.; Schicchi, N.; Fogante, M.; Agostini, A.; De Donato, M.C.; De Cataldo, C.; Giovagnoni, A.; Barile, A.; et al. Coronary artery disease (CAD) extension-derived risk stratification for asymptomatic diabetic patients: Usefulness of low-dose coronary computed tomography angiography (CCTA) in detecting high-risk profile patients. *Radiol. Med.* **2020**, *125*, 1249–1259. [[CrossRef](#)] [[PubMed](#)]
84. Agostini, A.; Borgheresi, A.; Carotti, M.; Ottaviani, L.; Badaloni, M.; Floridi, C.; Giovagnoni, A. Third-generation iterative reconstruction on a dual-source, high-pitch, low-dose chest CT protocol with tin filter for spectral shaping at 100 kV: A study on a small series of COVID-19 patients. *Radiol. Med.* **2021**, *126*, 388–398. [[CrossRef](#)]
85. Esposito, A.; Gallone, G.; Palmisano, A.; Marchitelli, L.; Catapano, F.; Francone, M. The current landscape of imaging recommendations in cardiovascular clinical guidelines: Toward an imaging-guided precision medicine. *Radiol. Med.* **2020**, *125*, 1013–1023. [[CrossRef](#)]
86. Cicero, G.; Ascenti, G.; Albrecht, M.H.; Blandino, A.; Cavallaro, M.; D’Angelo, T.; Carerj, M.L.; Vogl, T.J.; Mazziotti, S. Extra-abdominal dual-energy CT applications: A comprehensive overview. *Radiol. Med.* **2020**, *125*, 384–397. [[CrossRef](#)]
87. Leone, A.; Criscuolo, M.; Gulli, C.; Petrosino, A.; Bianco, N.C.; Colosimo, C. Systemic mastocytosis revisited with an emphasis on skeletal manifestations. *Radiol. Med.* **2021**, *126*, 585–598. [[CrossRef](#)]
88. Chalayer, E.; Tavernier-Tardy, E.; Clavreul, G.; Bay, J.-O.; Cornillon, J. Carcinomatosis lymphangitis and pleurisy after allo-SCT in two patients with secondary leukemia after breast cancer. *Bone Marrow Transplant.* **2012**, *47*, 155–156. [[CrossRef](#)] [[PubMed](#)]
89. Quigley, D.; Donnell, R.O.; McDonnell, C. Pulmonary lymphangitis sarcomatosis: A rare cause of severe progressive dyspnoea. *BMJ Case Rep.* **2022**, *15*, e246128. [[CrossRef](#)] [[PubMed](#)]
90. Souza, B.D.S.; Bonamigo, R.R.; Viapiana, G.L.; Cartell, A. Signet ring cells in carcinomatous lymphangitis due to gastric adenocarcinoma. *An. Bras. Dermatol.* **2020**, *95*, 490–492. [[CrossRef](#)] [[PubMed](#)]
91. Zieda, A.; Sbardella, S.; Patel, M.; Smith, R. Diagnostic Bias in the COVID-19 Pandemic: A Series of Short Cases. *Eur. J. Case Rep. Intern. Med.* **2021**, *8*, 002575. [[CrossRef](#)] [[PubMed](#)]
92. Giannakis, A.; Móre, D.; Erdmann, S.; Kintzelé, L.; Fischer, R.M.; Vogel, M.N.; Mangold, D.L.; von Stackelberg, O.; Schnitzler, P.; Zimmermann, S.; et al. COVID-19 pneumonia and its lookalikes: How radiologists perform in differentiating atypical pneumonias. *Eur. J. Radiol.* **2021**, *144*, 110002. [[CrossRef](#)] [[PubMed](#)]
93. Borghesi, A.; Sverzellati, N.; Polverosi, R.; Balbi, M.; Baratella, E.; Busso, M.; Calandriello, L.; Cortese, G.; Farchione, A.; Iezzi, R.; et al. Impact of the COVID-19 pandemic on the selection of chest imaging modalities and reporting systems: A survey of Italian radiologists. *Radiol. Med.* **2021**, *126*, 1258–1272. [[CrossRef](#)]
94. Weber, J.S.; D’Angelo, S.P.; Minor, D.; Hodi, S.F.; Gutzmer, R.; Neyns, B.; Hoeller, C.; Khushalani, N.I.; Miller, W.H., Jr.; Lao, C.D.; et al. Nivolumab versus chemotherapy in patients with advanced melanoma who progressed after anti-CTLA-4 treatment (CheckMate 037): A randomised, controlled, open-label, phase 3 trial. *Lancet Oncol.* **2015**, *16*, 375–384. [[CrossRef](#)]
95. Robert, C.; Ribas, A.; Wolchok, J.D.; Hodi, S.F.; Hamid, O.; Kefford, R.; Weber, J.S.; Joshua, A.M.; Hwu, W.-J.; Gangadhar, T.C.; et al. Anti-programmed-death-receptor-1 treatment with pembrolizumab in ipilimumab-refractory advanced melanoma: A randomised dose-comparison cohort of a phase 1 trial. *Lancet* **2014**, *384*, 1109–1117. [[CrossRef](#)]
96. Brahmer, J.; Reckamp, K.L.; Baas, P.; Crinò, L.; Eberhardt, W.E.E.; Poddubskaya, E.; Antonia, S.; Pluzanski, A.; Vokes, E.; Holgado, E.; et al. Nivolumab versus docetaxel in advanced squamous-cell non-small-cell lung cancer. *N. Engl. J. Med.* **2015**, *373*, 123–135. [[CrossRef](#)]
97. Borghaei, H.; Paz-Ares, L.; Horn, L.; Spigel, D.R.; Steins, M.; Ready, N.E.; Chow, L.Q.; Vokes, E.E.; Felip, E.; Holgado, E.; et al. Nivolumab versus docetaxel in advanced nonsquamous non-small-cell lung cancer. *N. Engl. J. Med.* **2015**, *373*, 1627–1639. [[CrossRef](#)]
98. Garon, E.B.; Rizvi, N.A.; Hui, R.; Leighl, N.; Balmanoukian, A.S.; Eder, J.P.; Patnaik, A.; Aggarwal, C.; Gubens, M.; Horn, L.; et al. Pembrolizumab for the treatment of non-small-cell lung cancer. *N. Engl. J. Med.* **2015**, *372*, 2018–2028. [[CrossRef](#)]
99. Herbst, R.S.; Baas, P.; Kim, D.W.; Felip, E.L.; Pérez-Gracia, J.L.; Han, J.-Y.; Molina, J.; Kim, J.-H.; Dubos Arvis, C.; Ahn, M.-J.; et al. Pembrolizumab versus docetaxel for previously treated, PD-L1-positive, advanced non-small-cell lung cancer (KEYNOTE-010): A randomised controlled trial. *Lancet* **2015**, *387*, 1540–1550. [[CrossRef](#)]
100. Motzer, R.J.; Escudier, B.; McDermott, D.F.; George, S.; Hammers, H.J.; Srinivas, S.; Tykodi, S.S.; Sosman, J.A.; Procopio, G.; Plimack, E.R.; et al. Nivolumab versus everolimus in advanced renal-cell carcinoma. *N. Engl. J. Med.* **2015**, *373*, 1803–1813. [[CrossRef](#)] [[PubMed](#)]
101. Ansell, S.M.; Lesokhin, A.M.; Borrello, I.; Halwani, A.; Scott, E.C.; Gutierrez, M.; Schuster, S.J.; Millenson, M.M.; Cattray, D.; Freeman, G.J.; et al. PD-1 blockade with nivolumab in relapsed or refractory Hodgkin’s lymphoma. *N. Engl. J. Med.* **2015**, *372*, 311–319. [[CrossRef](#)] [[PubMed](#)]
102. Rosenberg, J.E.; Hoffman-Censits, J.; Powles, T.; van der Heijden, M.S.; Balar, A.V.; Necchi, A.; Dawson, N.; O’Donnell, P.H.; Balmanoukian, A.; Loriot, Y.; et al. Atezolizumab in patients with locally advanced and metastatic urothelial carcinoma who have progressed following treatment with platinum-based chemotherapy: A single-arm, multicentre, phase 2 trial. *Lancet* **2016**, *387*, 1909–1920. [[CrossRef](#)]

103. Larkin, J.; Chiarion-Sileni, V.; Gonzalez, R.; Grob, J.J.; Cowey, L.; Lao, C.D.; Schadendorf, D.; Dummer, R.; Smylie, M.; Rutkowski, P.; et al. Combined nivolumab and ipilimumab or monotherapy in untreated melanoma. *N. Engl. J. Med.* **2015**, *373*, 23–34. [[CrossRef](#)] [[PubMed](#)]
104. Naidoo, J.; Page, D.B.; Li, B.T.; Connel, L.C.; Schindler, K.; Lacouture, M.E.; Postow, M.A.; Wolchok, J.D. Toxicities of the anti-PD-1 and anti-PD-L1 immune checkpoint antibodies. *Ann. Oncol.* **2015**, *26*, 2375–2391. [[CrossRef](#)]
105. Genestreti, G.; Di Battista, M.; Trisolini, R.; Denicolo, F.; Valli, M.; Agli, L.A.; dal Piaz, G.; de Biase, D.; Bartolotti, M.; Cavallo, G.; et al. A commentary on interstitial pneumonitis induced by docetaxel: Clinical cases and systematic review of the literature. *Tumori* **2015**, *101*, e92–e95. [[CrossRef](#)]
106. Poole, B.B.; Hamilton, L.A.; Brockman, M.M.; Brockman, M.M.; Byrd, D.C. Interstitial pneumonitis from treatment with gemcitabine. *Hosp. Pharm.* **2014**, *49*, 847–850. [[CrossRef](#)]
107. Comis, R.L. Bleomycin pulmonary toxicity: Current status and future directions. *Semin. Oncol.* **1992**, *19*, 64–70.
108. Ando, M.; Okamoto, I.; Yamamoto, N.; Takeda, K.; Tamura, K.; Seto, T.; Ariyoshi, Y.; Fukuoka, M. Predictive factors for interstitial lung disease, antitumor response, and survival in non-small-cell lung cancer patients treated with gefitinib. *J. Clin. Oncol.* **2006**, *24*, 2549–2556. [[CrossRef](#)] [[PubMed](#)]
109. Liu, V.; White, D.A.; Zakowski, M.F.; Travis, W.; Kris, M.G.; Ginsberg, M.S.; Miller, V.A.; Azzoli, C.G. Pulmonary toxicity associated with erlotinib. *Chest* **2007**, *132*, 1042–1044. [[CrossRef](#)] [[PubMed](#)]
110. White, D.A.; Camus, P.; Endo, M.; Escudier, B.; Calvo, E.; Akaza, H.; Uemura, H.; Kpamegan, E.; Kay, A.; Robson, M.; et al. Noninfectious pneumonitis after everolimus therapy for advanced renal cell carcinoma. *Am. J. Respir. Crit. Care Med.* **2010**, *182*, 396–403. [[CrossRef](#)] [[PubMed](#)]
111. Bradley, J.; Movsas, B. Radiation pneumonitis and esophagitis in thoracic irradiation. *Cancer Treat. Res.* **2006**, *128*, 43–64.
112. Weshler, Z.; Breuer, R.; Or, R.; Naparste, E.; Pfefer, M.R.; Lowenthal, E.; Slavin, S. Interstitial pneumonitis after total body irradiation: Effect of partial lung shielding. *Br. J. Haematol.* **1990**, *74*, 61–64. [[CrossRef](#)]
113. Palmucci, S.; Roccasalva, F.; Puglisi, S.; Torrisi, S.E.; Vindigni, V.; Mauro, L.A.; Ettorre, G.C.; Piccoli, M.; Vancheri, C. Clinical and radiological features of idiopathic interstitial pneumonias (IIPs): A pictorial review. *Insights Imaging* **2014**, *5*, 347–364. [[CrossRef](#)]
114. Khunger, M.; Rakshit, S.; Pasupuleti, V.; Hernandez, A.V.; Mazzone, P.; Stevenson, J.; Pennell, N.; Velcheti, V. Incidence of Pneumonitis with Use of Programmed Death 1 and Programmed Death-Ligand 1 Inhibitors in Non-Small Cell Lung Cancer: A Systematic Review and Meta-Analysis of Trials. *Chest* **2017**, *152*, 271–281. [[CrossRef](#)]
115. Khoja, L.; Day, D.; Chen, T.W.-W.; Siu, L.L.; Hansen, A.R. Tumour- and class-specific patterns of immune-related adverse events of immune checkpoint inhibitors: A systematic review. *Ann. Oncol.* **2017**, *28*, 2377–2385. [[CrossRef](#)]
116. Suresh, K.; Voong, K.R.; Shankar, B.; Forde, P.M.; Ettinger, D.S.; Marrone, K.A.; Kelly, R.J.; Hann, C.L.; Levy, B.; Feliciano, J.L.; et al. Pneumonitis in Non-Small Cell Lung Cancer Patients Receiving Immune Checkpoint Immunotherapy: Incidence and Risk Factors. *J. Thorac. Oncol.* **2018**, *13*, 1930–1939. [[CrossRef](#)]
117. Tay, R.Y.; Califano, R. Checkpoint Inhibitor Pneumonitis—Real-World Incidence and Risk. *J. Thorac. Oncol.* **2018**, *13*, 1812–1814. [[CrossRef](#)]
118. Kalisz, K.R.; Ramaiya, N.H.; Laukamp, K.R.; Gupta, A. Immune Checkpoint Inhibitor Therapy-related Pneumonitis: Patterns and Management. *RadioGraphics* **2019**, *39*, 1923–1937. [[CrossRef](#)] [[PubMed](#)]
119. Bianchi, A.; Mazzoni, L.N.; Busoni, S.; Pinna, N.; Albanesi, M.; Cavigli, E.; Cozzi, D.; Poggesi, A.; Miele, V.; Fainardi, E.; et al. Assessment of cerebrovascular disease with computed tomography in COVID-19 patients: Correlation of a novel specific visual score with increased mortality risk. *Radiol. Med.* **2021**, *126*, 570–576. [[CrossRef](#)] [[PubMed](#)]
120. Cartocci, G.; Colaiacomo, M.C.; Lanciotti, S.; Andreoli, C.; De Cicco, M.L.; Brachetti, G.; Pugliese, S.; Capoccia, L.; Tortora, A.; Scala, A.; et al. Correction to: Chest CT for early detection and management of coronavirus disease (COVID-19): A report of 314 patients admitted to Emergency Department with suspected pneumonia. *Radiol. Med.* **2020**, *126*, 642. [[CrossRef](#)] [[PubMed](#)]
121. Zompatori, M.; Poletti, V.; Battista, G.; Schiavina, M.; Fadda, E.; Tetta, C. Diffuse cystic lung disease in the adult patient. *Radiol. Med.* **2000**, *99*, 12–21.
122. Delaunay, M.; Cadranet, J.; Lusque, A.; Meyer, N.; Gounaut, V.; Moro-Sibilot, D.; Michot, J.-M.; Raimbourg, J.; Girard, N.; Guisier, F.; et al. Immune-checkpoint inhibitors associated with interstitial lung disease in cancer patients. *Eur. Respir. J.* **2017**, *50*, 1700050. [[CrossRef](#)]
123. Teng, F.; Li, M.; Yu, J. Radiation recall pneumonitis induced by PD-1/PD-L1 blockades: Mechanisms and therapeutic implications. *BMC Med.* **2020**, *18*, 275. [[CrossRef](#)]
124. Cousin, F.; Desir, C.; Ben Mustapha, S.; Mievis, C.; Coucke, P.; Hustinx, R. Incidence, risk factors, and CT characteristics of radiation recall pneumonitis induced by immune checkpoint inhibitor in lung cancer. *Radiother. Oncol.* **2021**, *157*, 47–55. [[CrossRef](#)]
125. D’Agostino, V.; Caranci, F.; Negro, A.; Piscitelli, V.; Tuccillo, B.; Fasano, F.; Sirabella, G.; Marano, I.; Granata, V.; Grassi, R.; et al. A Rare Case of Cerebral Venous Thrombosis and Disseminated Intravascular Coagulation Temporally Associated to the COVID-19 Vaccine Administration. *J. Pers. Med.* **2021**, *11*, 285. [[CrossRef](#)]
126. Girometti, R.; Linda, A.; Conte, P.; Lorenzon, M.; De Serio, I.; Jerman, K.; Londero, V.; Zuiani, C. Multireader comparison of contrast-enhanced mammography versus the combination of digital mammography and digital breast tomosynthesis in the preoperative assessment of breast cancer. *Radiol. Med.* **2021**, *126*, 1407–1414. [[CrossRef](#)]

127. Gerasia, R.; Mamone, G.; Amato, S.; Cucchiara, A.; Gallo, G.S.; Tafaro, C.; Fiorello, G.; Caruso, C.; Miraglia, R. COVID-19 safety measures at the Radiology Unit of a Transplant Institute: The non-COVID-19 patient's confidence with safety procedures. *Radiol. Med.* **2022**, *13*, 426–432. [[CrossRef](#)]
128. McGovern, K.; Ghaly, M.; Esposito, M.; Barnaby, K.; Seetharamu, N. Radiation recall pneumonitis in the setting of immunotherapy and radiation: A focused review. *Futur. Sci. OA* **2019**, *5*, FSO378. [[CrossRef](#)] [[PubMed](#)]
129. Cellini, F.; Di Franco, R.; Manfreda, S.; Borzillo, V.; Maranzano, E.; Pergolizzi, S.; Morganti, A.G.; Fusco, V.; Deodato, F.; Santarelli, M.; et al. Palliative radiotherapy indications during the COVID-19 pandemic and in future complex logistic settings: The NORMALITY model. *Radiol. Med.* **2021**, *126*, 1619–1656. [[CrossRef](#)] [[PubMed](#)]
130. De Felice, F.; Boldrini, L.; Greco, C.; Nardone, V.; Salvestrini, V.; Desideri, I. ESTRO vision 2030: The young Italian Association of Radiotherapy and Clinical Oncology (yAIRO) commitment statement. *Radiol. Med.* **2021**, *126*, 1374–1376. [[CrossRef](#)] [[PubMed](#)]
131. Bellardita, L.; Colciago, R.R.; Frasca, S.; De Santis, M.C.; Gay, S.; Palorini, F.; La Rocca, E.; Valdagni, R.; Rancati, T.; Lozza, L. Breast cancer patient perspective on opportunities and challenges of a genetic test aimed to predict radio-induced side effects before treatment: Analysis of the Italian branch of the REQUITE project. *Radiol. Med.* **2021**, *126*, 1366–1373. [[CrossRef](#)]
132. Merlotti, A.; Bruni, A.; Borghetti, P.; Ramella, S.; Scotti, V.; Trovò, M.; Chiari, R.; Lohr, F.; Ricardi, U.; Bria, E.; et al. Sequential chemo-hypofractionated RT versus concurrent standard CRT for locally advanced NSCLC: GRADE recommendation by the Italian Association of Radiotherapy and Clinical Oncology (AIRO). *Radiol. Med.* **2021**, *126*, 1117–1128. [[CrossRef](#)]
133. Afacan, E.; Ögüt, B.; Üstün, P.; Şentürk, E.; Yazıcı, O.; Adışen, E. Radiation recall dermatitis triggered by inactivated COVID-19 vaccine. *Clin. Exp. Dermatol.* **2021**, *46*, 1582–1584. [[CrossRef](#)]
134. Masci, G.M.; Iafrate, F.; Ciccarella, F.; Pambianchi, G.; Panebianco, V.; Pasculli, P.; Ciardi, M.R.; Mastroianni, C.M.; Ricci, P.; Catalano, C.; et al. Tocilizumab effects in COVID-19 pneumonia: Role of CT texture analysis in quantitative assessment of response to therapy. *Radiol. Med.* **2021**, *126*, 1170–1180. [[CrossRef](#)]
135. Francolini, G.; Desideri, I.; Stocchi, G.; Ciccone, L.P.; Salvestrini, V.; Garlatti, P.; Aquilano, M.; Greto, D.; Bonomo, P.; Meattini, I.; et al. Impact of COVID-19 on workload burden of a complex radiotherapy facility. *Radiol. Med.* **2021**, *126*, 717–721. [[CrossRef](#)]
136. Rivera, D.T.; Misra, A.; Sanil, Y.; Sabzghabaei, N.; Safa, R.; Garcia, R.U. Vitamin D and morbidity in children with Multisystem inflammatory syndrome related to COVID-19. *Prog. Pediatr. Cardiol.* **2022**, 101507. [[CrossRef](#)]
137. Chua, G.T.; Wong, J.S.; Chung, J.; Lam, I.; Kwong, J.; Leung, K.; Law, C.; Lam, C.; Kwok, J.; Chu, P.W.; et al. Paediatric multisystem inflammatory syndrome temporally associated with SARS-CoV-2: A case report. *Hong Kong Med. J.* **2022**, *28*, 76–78. [[CrossRef](#)]
138. Barrezueta, L.B.; Raposo, M.B.; Fernández, I.S.; Casillas, P.L.; Francisco, C.V.; Vázquez, A.P. Impact of the COVID-19 pandemic on admissions for respiratory infections in the Pediatric Intensive Care Unit. *Med. Intensiv.* **2022**. [[CrossRef](#)] [[PubMed](#)]
139. Kovács, A.; Palásti, P.; Veréb, D.; Bozsik, B.; Palkó, A.; Kincses, Z.T. The sensitivity and specificity of chest CT in the diagnosis of COVID-19. *Eur. Radiol.* **2021**, *31*, 2819–2824. [[CrossRef](#)] [[PubMed](#)]
140. De Felice, F.; D'Angelo, E.; Ingargiola, R.; Iacovelli, N.A.; Alterio, D.; Franco, P.; Bonomo, P.; Merlotti, A.; Bacigalupo, A.; Maddalo, M.; et al. A snapshot on radiotherapy for head and neck cancer patients during the COVID-19 pandemic: A survey of the Italian Association of Radiotherapy and Clinical Oncology (AIRO) head and neck working group. *Radiol. Med.* **2020**, *126*, 343–347. [[CrossRef](#)] [[PubMed](#)]
141. Katal, S.; Johnston, S.K.; Johnston, J.H.; Gholamrezanezhad, A. Imaging Findings of SARS-CoV-2 Infection in Pediatrics: A Systematic Review of Coronavirus Disease 2019 (COVID-19) in 850 Patients. *Acad. Radiol.* **2020**, *27*, 1608–1621. [[CrossRef](#)] [[PubMed](#)]
142. Fichera, G.; Stramare, R.; De Conti, G.; Motta, R.; Giraud, C. It's not over until it's over: The chameleonic behavior of COVID-19 over a six-day period. *Radiol. Med.* **2020**, *125*, 514–516. [[CrossRef](#)]
143. Moroni, C.; Bindi, A.; Cavigli, E.; Cozzi, D.; Luvarà, S.; Smorchkova, O.; Zantonelli, G.; Miele, V.; Bartolucci, M. CT findings of non-neoplastic central airways diseases. *Jpn. J. Radiol.* **2021**, *40*, 107–119. [[CrossRef](#)]
144. Boger, B.; Fachi, M.M.; Vilhena, R.O.; Cobre, A.F.; Tonin, F.; Pontarolo, R. Systematic review with meta-analysis of the accuracy of diagnostic tests for COVID-19. *Am. J. Infect. Control* **2020**, *49*, 21–29. [[CrossRef](#)]
145. Khatami, F.; Saatchi, M.; Zadeh, S.S.T.; Aghamir, Z.S.; Shabestari, A.N.; Reis, L.O.; Aghamir, S.M.K. A meta-analysis of accuracy and sensitivity of chest CT and RT-PCR in COVID-19 diagnosis. *Sci. Rep.* **2020**, *10*, 22402. [[CrossRef](#)]
146. Waller, J.V.; Allen, I.E.; Lin, K.K.; Diaz, M.J.; Henry, T.S.; Hope, M.D. The Limited Sensitivity of Chest Computed Tomography Relative to Reverse Transcription Polymerase Chain Reaction for Severe Acute Respiratory Syndrome Coronavirus-2 Infection: A systematic review on COVID-19 diagnostics. *Investig. Radiol.* **2020**, *55*, 754–761. [[CrossRef](#)]
147. Islam, N.; Ebrahimzadeh, S.; Salameh, J.-P.; Kazi, S.; Fabiano, N.; Treanor, L.; Absi, M.; Hallgrimson, Z.; Leeflang, M.M.; Hooft, L.; et al. Thoracic imaging tests for the diagnosis of COVID-19. *Cochrane Database Syst. Rev.* **2021**, *2021*, CD013639. [[CrossRef](#)]
148. Bernheim, A.; Mei, X.; Huang, M.; Yang, Y.; Fayad, Z.A.; Zhang, N.; Diao, K.; Lin, B.; Zhu, X.; Li, K.; et al. Chest CT Findings in Coronavirus Disease-19 (COVID-19): Relationship to Duration of Infection. *Radiology* **2020**, *295*, 200463. [[CrossRef](#)] [[PubMed](#)]
149. Caruso, D.; Zerunian, M.; Polici, M.; Pucciarelli, F.; Polidori, T.; Rucci, C.; Guido, G.; Bracci, B.; De Dominicis, C.; Laghi, A. Chest CT Features of COVID-19 in Rome, Italy. *Radiology* **2020**, *296*, E79–E85. [[CrossRef](#)] [[PubMed](#)]
150. Ye, Z.; Zhang, Y.; Wang, Y.; Huang, Z.; Song, B. Chest CT manifestations of new coronavirus disease 2019 (COVID-19): A pictorial review. *Eur. Radiol.* **2020**, *30*, 4381–4389. [[CrossRef](#)] [[PubMed](#)]

151. Pan, F.; Ye, T.; Sun, P.; Gui, S.; Liang, B.; Li, L.; Zheng, D.; Wang, J.; Hesketh, R.L.; Yang, L.; et al. Time Course of Lung Changes at Chest CT during Recovery from Coronavirus Disease 2019 (COVID-19). *Radiology* **2020**, *295*, 715–721. [[CrossRef](#)]
152. Bai, H.X.; Hsieh, B.; Xiong, Z.; Halsey, K.; Choi, J.W.; Tran, T.M.L.; Pan, I.; Shi, L.-B.; Wang, D.-C.; Mei, J.; et al. Performance of Radiologists in Differentiating COVID-19 from Non-COVID-19 Viral Pneumonia at Chest CT. *Radiology* **2020**, *296*, 200823. [[CrossRef](#)]
153. Neri, E.; Coppola, F.; Miele, V.; Bibbolino, C.; Grassi, R. Artificial intelligence: Who is responsible for the diagnosis? *Radiol. Med.* **2020**, *125*, 517–521. [[CrossRef](#)]
154. van Assen, M.; Muscogiuri, G.; Caruso, D.; Lee, S.J.; Laghi, A.; De Cecco, C.N. Artificial intelligence in cardiac radiology. *Radiol. Med.* **2020**, *125*, 1186–1199. [[CrossRef](#)]
155. Hu, H.-T.; Shan, Q.-Y.; Chen, S.-L.; Li, B.; Feng, S.-T.; Xu, E.-J.; Li, X.; Long, J.-Y.; Xie, X.-Y.; Lu, M.-D.; et al. CT-based radiomics for preoperative prediction of early recurrent hepatocellular carcinoma: Technical reproducibility of acquisition and scanners. *Radiol. Med.* **2020**, *125*, 697–705. [[CrossRef](#)]
156. Loffi, M.; Regazzoni, V.; Toselli, M.; Cereda, A.; Palmisano, A.; Vignale, D.; Moroni, F.; Pontone, G.; Andreini, D.; Mancini, E.M.; et al. Incidence and characterization of acute pulmonary embolism in patients with SARS-CoV-2 pneumonia: A multicenter Italian experience. *PLoS ONE* **2021**, *22*, e0245565. [[CrossRef](#)]
157. Zhang, L.; Kang, L.; Li, G.; Zhang, X.; Ren, J.; Shi, Z.; Li, J.; Yu, S. Computed tomography-based radiomics model for discriminating the risk stratification of gastrointestinal stromal tumors. *Radiol. Med.* **2020**, *125*, 465–473. [[CrossRef](#)]
158. Bracci, S.; Dolciami, M.; Trobiani, C.; Izzo, A.; Pernazza, A.; D’Amati, G.; Manganaro, L.; Ricci, P. Quantitative CT texture analysis in predicting PD-L1 expression in locally advanced or metastatic NSCLC patients. *Radiol. Med.* **2021**, *126*, 1425–1433. [[CrossRef](#)] [[PubMed](#)]
159. Qin, H.; Que, Q.; Lin, P.; Li, X.; Wang, X.-R.; He, Y.; Chen, J.-Q.; Yang, H. Magnetic resonance imaging (MRI) radiomics of papillary thyroid cancer (PTC): A comparison of predictive performance of multiple classifiers modeling to identify cervical lymph node metastases before surgery. *Radiol. Med.* **2021**, *126*, 1312–1327. [[CrossRef](#)] [[PubMed](#)]
160. Kirienko, M.; Ninatti, G.; Cozzi, L.; Voulaz, E.; Gennaro, N.; Barajon, I.; Ricci, F.; Carlo-Stella, C.; Zucali, P.; Sollini, M.; et al. Computed tomography (CT)-derived radiomic features differentiate prevascular mediastinum masses as thymic neoplasms versus lymphomas. *Radiol. Med.* **2020**, *125*, 951–960. [[CrossRef](#)] [[PubMed](#)]
161. Farchione, A.; Larici, A.R.; Masciocchi, C.; Cicchetti, G.; Congedo, M.T.; Franchi, P.; Gatta, R.; Cicero, S.L.; Valentini, V.; Bonomo, L.; et al. Exploring technical issues in personalized medicine: NSCLC survival prediction by quantitative image analysis—Usefulness of density correction of volumetric CT data. *Radiol. Med.* **2020**, *125*, 625–635. [[CrossRef](#)]
162. D’Angelo, A.; Orlandi, A.; Bufi, E.; Mercogliano, S.; Belli, P.; Manfredi, R. Automated breast volume scanner (ABVS) compared to handheld ultrasound (HHUS) and contrast-enhanced magnetic resonance imaging (CE-MRI) in the early assessment of breast cancer during neoadjuvant chemotherapy: An emerging role to monitoring tumor response? *Radiol. Med.* **2021**, *126*, 517–526. [[CrossRef](#)]
163. Kassania, S.H.; Kassanib, P.H.; Wesolowskic, M.J.; Schneidera, K.A.; Detersa, R. Automatic Detection of Coronavirus Disease (COVID-19) in X-ray and CT Images: A Machine Learning Based Approach. *Biocybern. Biomed. Eng.* **2021**, *41*, 867–879. [[CrossRef](#)]
164. Barbosa, E.J.M.; Georgescu, B.; Chaganti, S.; Aleman, G.B.; Cabrero, J.B.; Chabin, G.; Flohr, T.; Grenier, P.; Grbic, S.; Gupta, N.; et al. Machine learning automatically detects COVID-19 using chest CTs in a large multicenter cohort. *Eur. Radiol.* **2021**, *31*, 8775–8785. [[CrossRef](#)]
165. Giordano, F.; Ippolito, E.; Quattrocchi, C.; Greco, C.; Mallio, C.; Santo, B.; D’Alessio, P.; Crucitti, P.; Fiore, M.; Zobel, B.; et al. Radiation-Induced Pneumonitis in the Era of the COVID-19 Pandemic: Artificial Intelligence for Differential Diagnosis. *Cancers* **2021**, *13*, 1960. [[CrossRef](#)]
166. Bai, H.X.; Wang, R.; Xiong, Z.; Hsieh, B.; Chang, K.; Halsey, K.; Tran, T.M.L.; Choi, J.W.; Wang, D.-C.; Shi, L.-B.; et al. Artificial Intelligence Augmentation of Radiologist Performance in Distinguishing COVID-19 from Pneumonia of Other Origin at Chest CT. *Radiology* **2020**, *296*, E156–E165. [[CrossRef](#)]
167. Granata, V.; Fusco, R.; Vallone, P.; Setola, S.V.; Picone, C.; Grassi, F.; Patrone, R.; Belli, A.; Izzo, F.; Petrillo, A. Not only lymphadenopathy: Case of chest lymphangitis assessed with MRI after COVID 19 vaccine. *Infect. Agents Cancer* **2022**, *17*, 8. [[CrossRef](#)]
168. Ozsahin, I.; Sekeroglu, B.; Musa, M.S.; Mustapha, M.T.; Ozsahin, D.U. Review on Diagnosis of COVID-19 from Chest CT Images Using Artificial Intelligence. *Comput. Math. Methods Med.* **2020**, *2020*, 9756518. [[CrossRef](#)] [[PubMed](#)]